Effects of Nuclear Hyperfine Mixing on $^{229}Th^{3+}$ Ions

Jie Zhou and Xu Wang*
Graduate School, China Academy of Engineering Physics, Beijing 100193, China

(Received 28 December 2024; revised 21 October 2025; accepted 17 February 2026; published 4 March 2026)

The triply charged thorium-229 ion ($^{229}Th^{3+}$) has been identified as a promising candidate for the development of ultraprecise nuclear clocks. In this Letter, we investigate how the electron structure of this ion, particularly the single valence electron, influences the nucleus through nuclear hyperfine mixing (NHM)—a phenomenon previously studied almost solely for highly charged ions. We show that NHM opens electric dipole ($E1$) transition channels, which can significantly enhance the efficiency of nuclear isomeric excitation by 2 orders of magnitude. Additionally, NHM accelerates the spontaneous decay rate of the nuclear isomeric state by 1% to 7%, depending on the specific hyperfine level involved.

DOI: 10.1103/8jhh-ktfy

Introduction—The ^{229}Th nucleus has a unique low-lying isomeric state approximately 8.4 eV above the nuclear ground state [1–6], and it has been proposed to use the transition between these two states to construct nuclear clocks [7] that have certain advantages over atomic clocks based on electronic transitions [8,9]. Substantial progress has been made on the properties of this nucleus [10–13] and on methods of isomeric excitation [14–25]. In particular, direct optical excitations have been achieved recently by three groups using ^{229}Th-doped crystals [26–28].

^{229}Th nuclear clocks may be realized along the following approaches: (1) crystal nuclear clocks with ^{229}Th embedded in crystals [26–31]; (2) ionic nuclear clocks with ^{229}Th ions (especially the $^{229}Th^{3+}$ ion which is convenient for laser cooling) confined in ion traps [7,32–35]; and (3) internal conversion nuclear clocks with ^{229}Th adhered on the surface of a substrate or in low-bandgap materials [36,37]. Each approach has its pros and cons. The crystal approach provides a large number of participating ^{229}Th nuclei (doped density $\sim 10^{18}$ cm^{-3}), but the complex electronic and phononic environment may limit the accuracy. The ionic approach provides the cleanest environment with the highest anticipated accuracy, but the number of trapped ions is very limited ($\sim 100 - 1000$) [38]. Therefore it is extremely challenging to achieve direct optical excitation. Significant recent progress has been mainly along the crystal approach [26–28]. Nevertheless, important advances have also been seen along the ionic approach. For example, Yamaguchi *et al.* were able to confine $^{229}Th^{3+}$ ions in a linear Paul trap for over half an hour and measured the isomeric lifetime in an isolated environment [13].

The goal of the current Letter is to contribute to the ionic approach by providing previously unknown and unexpected theoretical insights into the $^{229}Th^{3+}$ ion. Specifically, we show effects of nuclear hyperfine mixing (NHM) on this ionic state. These effects are unexpected because NHM is believed to be significant mostly for highly charged ions [39–42], such as $^{229}Th^{89+}$, $^{229}Th^{87+}$, $^{205}Pb^{77+}$, etc. In contrast, the influence of outer-shell electrons on the nucleus is much weaker for lowly charged ions such as $^{229}Th^{3+}$ [43–45] and it is unknown to what degree the ionic nuclear clock would be affected by NHM. In this Letter, we show that NHM opens new electric dipole ($E1$) transition channels that are otherwise forbidden. These $E1$ channels facilitate more efficient isomeric excitation by 2 orders of magnitude compared to the normal magnetic dipole ($M1$) transition. Additionally, we find that the NHM effect decreases the lifetime of the nuclear isomeric state by 1% to 7%, depending on the specific hyperfine level involved.

Theory of NHM—In an ion, the electrons generate a strong electromagnetic field at the site of the nucleus, causing mixing of nuclear states. This is NHM, which is also termed "spin mixing in hyperfine fields" in early literature [46–48]. The total Hamiltonian of a $^{229}Th^{3+}$ ion can be written as $H = H_e + H_n + H_{en}$, where H_e, H_n, H_{en} are the Hamiltonian for the electrons, for the nucleus, and for electron-nucleus interaction, respectively. The $^{229}Th^{3+}$ ion consists of a closed electronic shell and a single valence electron, and the closed electronic shell does not have hyperfine interaction with the nucleus, therefore H_e is taken as an effective Hamiltonian that yields correct fine structures of the valence electron. The noncentral electron-nucleus interaction H_{en} can be written with electric ($\tau = E$) and magnetic (M) λ-order irreducible tensor operators [49] as

$$H_{en} = \sum_{\tau=E,M} \sum_{\lambda\nu} \frac{4\pi}{2\lambda+1} (-1)^{\nu} \mathcal{M}_n^{(\tau\lambda\nu)} \mathcal{N}_e^{(\tau\lambda-\nu)}. \quad (1)$$

*Contact author: xwang@gscaep.ac.cn

Here, the nuclear multipole moment operator $\mathcal{M}_{\rm n}^{(\tau\lambda\nu)}$ is given explicitly as

$$\mathcal{M}_{\rm n}^{(E\lambda\nu)} = \int r^{\lambda}\rho_{\rm n}(\mathbf{r})Y_{\lambda\nu}(\theta,\phi)\mathrm{d}^3\mathbf{r}, \tag{2}$$

$$\mathcal{M}_{\rm n}^{(M\lambda\nu)} = -\frac{i}{c(\lambda+1)}\int r^{\lambda}\boldsymbol{j}_{\rm n}(\mathbf{r})\cdot\boldsymbol{L}Y_{\lambda\nu}(\theta,\phi)\mathrm{d}^3\mathbf{r}, \tag{3}$$

where Y is the spherical harmonic function, c is the speed of light, $\boldsymbol{L}$ is the angular momentum operator, and $\rho_{\rm n}$ and $\boldsymbol{j}_{\rm n}$ are the charge and current density operators of the nucleus. Operator $\mathcal{M}_{\rm e}^{(\tau\lambda\nu)}$ has the same form as $\mathcal{M}_{\rm n}^{(\tau\lambda\nu)}$, except that $\rho_{\rm n}$ and $\boldsymbol{j}_{\rm n}$ in Eqs. (2) and (3) are replaced with $\rho_{\rm e}$ and $\boldsymbol{j}_{\rm e}$ which are charge and current density operators of the electron. A total transition operator of the ion is defined as the sum of the nuclear and electronic transition operators: $\mathcal{M}^{(\tau\lambda\nu)} = \mathcal{M}_{\rm n}^{(\tau\lambda\nu)} + \mathcal{M}_{\rm e}^{(\tau\lambda\nu)}$. The corresponding "reduced" operators, including $\mathcal{M}_{\rm n}^{(\tau\lambda)}$, $\mathcal{M}_{\rm e}^{(\tau\lambda)}$, $\mathcal{M}^{(\tau\lambda)}$, are also useful in situations where the magnetic quantum number ν is summed over. The multipole operator $\mathcal{N}_{\rm e}^{(\tau\lambda\nu)}$ in Eq. (1) has a different form

$$\mathcal{N}_{\rm e}^{(E\lambda\nu)} = \int r^{-\lambda-1}\rho_{\rm e}(\mathbf{r})Y_{\lambda\nu}(\theta,\phi)\mathrm{d}^3\mathbf{r}, \tag{4}$$

$$\mathcal{N}_{\rm e}^{(M\lambda\nu)} = \frac{i}{c\lambda}\int r^{-\lambda-1}\boldsymbol{j}_{\rm e}(\mathbf{r})\cdot\boldsymbol{L}Y_{\lambda\nu}(\theta,\phi)\mathrm{d}^3\mathbf{r}, \tag{5}$$

and $\mathcal{N}_{\rm e}^{(\tau\lambda\nu)}$ only operates on the electron.

Without $H_{\rm en}$, the nucleus and the electron are independent from each other and the eigenstates of the system are a direct product of the nuclear states and the electronic states. With $H_{\rm en}$, hyperfine splitting happens and the energy levels are determined by the total angular momentum F which is coupled by the nuclear spin I and the electron angular momentum J. However, it is to be noted that a total-angular-momentum state $|i\rangle \equiv |I_i J_i F_i\rangle$ is not exactly the eigenstate. The rigorous eigenstate can be written as

$$|i\rangle_+ = a_i|i\rangle + \sum_j b_{ij}|j\rangle, \tag{6}$$

that is, mixing with state $|j\rangle = |I_j J_j F_j\rangle$ is possible. Here, the "+" sign in the subscript denotes an ion eigenstate with NHM included. Usually $a_i \approx 1$ and the mixing coefficient b_{ij} ($\ll 1$) can be calculated using perturbation theory as [42]

$$b_{ij} \approx \frac{\langle j|H_{\rm en}|i\rangle}{E_i - E_j} = \sum_{\tau\lambda}\frac{4\pi}{2\lambda+1}(-1)^{I_i+J_j+F_i}\begin{Bmatrix} I_i & J_i & F_j \\ J_j & I_j & \lambda \end{Bmatrix} \cdot \frac{\langle I_j\|\mathcal{M}_{\rm n}^{(\tau\lambda)}\|I_i\rangle\langle\gamma_j J_j\|\mathcal{N}_{\rm e}^{(\tau\lambda)}\|\gamma_i J_i\rangle}{E_i - E_j} \tag{7}$$

where $E_{i/j}$ is the energy of state $|i/j\rangle$, $\langle I_j\|\mathcal{M}_{\rm n}^{(\tau\lambda)}\|I_i\rangle$ is the reduced nuclear transition matrix element, and $\langle\gamma_j J_j\|\mathcal{N}_{\rm e}^{(\tau\lambda)}\|\gamma_i J_i\rangle$ is the reduced electronic transition matrix element with γ denoting all other electronic quantum numbers. If $I_i \neq I_j$ and $b_{ij} \neq 0$, different nuclear states are mixed and this is NHM.

NHM is closely related to, yet distinct from, the hyperfine quenching (HQ) process in atomic physics [50–57]. Both phenomena arise because the true eigenstates of an ion are hyperfine states, which can involve admixtures of different components. The essential difference is that HQ involves a single nuclear state, whereas NHM couples two (or more) nuclear states, thus enabling control over transitions between nuclear levels.

Opening of E1 nuclear excitation channels—The spin and parity of the nuclear ground (isomeric) state is $I_g^{\pi} = 5/2^+$ ($I_m^{\pi} = 3/2^+$), so the nuclear transition is of type $M1$ or $E2$. The electronic ground state of the $^{229}\mathrm{Th}^{3+}$ ion is $5f_{5/2}$ (hyperfine level $F = 3$).

NHM opens $E1$ nuclear excitation channels. For example, Fig. 1 shows the transition from the ground state of the ion, $|I_g, 5f_{5/2}\rangle_+$, to the excited state $|I_m, 6d_{3/2}\rangle_+$. Let us write down the expansions of these two states (both for $F = 3$):

$$|I_g, 5f_{5/2}\rangle_+ \approx |I_g, 5f_{5/2}\rangle + b_1|I_g, 5f_{7/2}\rangle + b_2|I_g, 6f_{5/2}\rangle + b_3|I_m, 5f_{5/2}\rangle + \ldots, \tag{8}$$

$$|I_m, 6d_{3/2}\rangle_+ \approx |I_m, 6d_{3/2}\rangle + \beta_1|I_m, 6d_{5/2}\rangle + \beta_2|I_m, 7d_{5/2}\rangle + \beta_3|I_g, 6d_{5/2}\rangle + \ldots, \tag{9}$$

where the values of the mixing coefficients are $b_1 = 1.9\times10^{-6}$, $b_2 = 7.0\times10^{-8}$, $b_3 = -2.1\times10^{-7}$, and $\beta_1 = -1.2\times10^{-5}$, $\beta_2 = -2.9\times10^{-7}$, $\beta_3 = -8.6\times10^{-8}$. All the states in the above expansions are for the $F = 3$ hyperfine level. One sees that the ground state is mixed with a small fraction of the nuclear excited state (the component with coefficient b_3), and the excited state is mixed with a small portion of the nuclear ground state (the component with coefficient β_3). Then we get a nonzero $E1$ transition matrix element

$$\begin{aligned} &{}_+\langle I_m, 6d_{3/2}|\mathcal{M}^{(E1\nu)}|I_g, 5f_{5/2}\rangle_+ \\ &\approx b_3\langle I_m, 6d_{3/2}|\mathcal{M}^{(E1\nu)}|I_m, 5f_{5/2}\rangle \\ &\quad + \beta_3\langle I_g, 6d_{5/2}|\mathcal{M}^{(E1\nu)}|I_g, 5f_{5/2}\rangle, \end{aligned} \tag{10}$$

where the total transition operator $\mathcal{M}^{(E1\nu)}$ is the sum of the nuclear and electronic transition operators, as mentioned above.

Note that this kind of $E1$ transition channel is possible only because of the NHM effect, without which the mixing coefficients $b_{1,2,3,\ldots}$ or $\beta_{1,2,3,\ldots}$ vanish and the above matrix

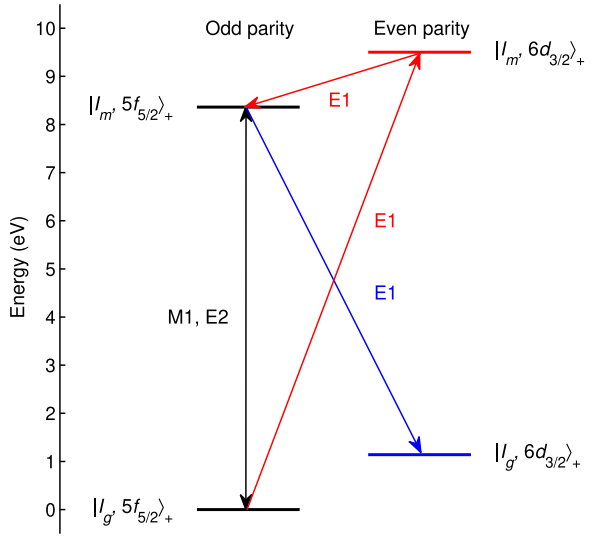

FIG. 1. Example $E1$ transition channels in the $^{229}Th^{3+}$ ion. The transition from $|I_g, 5f_{5/2}\rangle_+$ to $|I_m, 6d_{3/2}\rangle_+$ is an $E1$ transition with nuclear excitation opened by NHM. The transition from $|I_m, 5f_{5/2}\rangle_+$ to $|I_g, 6d_{3/2}\rangle_+$ is an $E1$ transition with nuclear decay opened by NHM. The transition from $|I_m, 6d_{3/2}\rangle_+$ to $|I_m, 5f_{5/2}\rangle_+$ is a purely electronic $E1$ decay. The transition between $|I_g, 5f_{5/2}\rangle_+$ and $|I_m, 5f_{5/2}\rangle_+$ is of types $M1$ and $E2$.

element vanishes. Without NHM, the transition from $|I_g, 5f_{5/2}\rangle$ to $|I_m, 6d_{3/2}\rangle$ cannot be accomplished directly. Instead, it is a second-order perturbative process that must go through an intermediate state, e.g., $\langle I_m, 6d_{3/2}|\mathcal{M}^{(E1\nu)}|I_m, 5f_{5/2}\rangle\langle I_m, 5f_{5/2}|\mathcal{M}^{(M1\nu')}|I_g, 5f_{5/2}\rangle$.

The transition from $|I_g, 5f_{5/2}\rangle_+$ to $|I_m, 5f_{5/2}\rangle_+$ is an $M1/E2$ ($M1$ dominant) process even with the NHM effect. This is because only states with the same parity can be mixed. Both of these states have odd parity, so only odd-parity states can be mixed into each state. There are no even-parity components that allow an $E1$ transition, which requires parity flipping.

More efficient pathway for isomeric excitation—The reduced $M1$ transition matrix element $_+\langle I_m, 5f_{5/2}\|\mathcal{M}^{(M1)}\|I_g, 5f_{5/2}\rangle_+$ is calculated to be 3.73×10^{-9} a.u., whereas the reduced $E1$ transition matrix element $_+\langle I_m, 6d_{3/2}\|\mathcal{M}^{(E1)}\|I_g, 5f_{5/2}\rangle_+$ is calculated to be 6.22×10^{-8} a.u., which is an order of magnitude higher. This leads to a nuclear isomeric excitation efficiency 2 orders of magnitude higher.

The excitation energy of the $M1$ channel is 8.356 eV (corresponding to a laser wavelength of 148 nm), and the excitation energy of the $E1$ channel is 9.497 eV (131 nm), which is 1.141 eV higher due to the accompanied electronic transition. In our calculation, the reduced nuclear transition probabilities are taken to be $B(M1, m \to g) = 0.0076$ W.u. and $B(E2, m \to g) = 27$ W.u. [58]. The electronic levels are calculated based on Dirac equations using the GRASP-2K package [59], and the levels with energies below 20 eV relative to the $5f_{5/2}$ ground state are listed in Table I. Our results agree well with existing data [60,61].

TABLE I. Partial electronic states in our calculation.

Odd parity	Energy (eV)	Even parity	Energy (eV)
$5f_{5/2}$	0	$6d_{3/2}$	1.141
$5f_{7/2}$	0.536	$6d_{5/2}$	1.798
$7p_{1/2}$	7.474	$7s_{1/2}$	2.869
$7p_{3/2}$	9.064	$8s_{1/2}$	14.841
$8p_{1/2}$	15.549	$7d_{3/2}$	14.849
$6f_{5/2}$	15.791	$7d_{5/2}$	15.065
$6f_{7/2}$	15.859	$5g_{9/2}$	19.772
$8p_{3/2}$	17.354	$5g_{7/2}$	19.776

The probability of isomeric excitation can be calculated using the following formula for $M1$ or $E1$ transitions:

$$P_{\mathrm{exc}}(t) \approx \frac{|_+\langle f\|\mathcal{M}^{(\tau 1)}\|i\rangle_+|^2}{3(2F_i+1)} It^2, \tag{11}$$

where F_i is the total angular momentum quantum number of the initial state $|i\rangle_+$, I is the laser intensity, and t is the time of laser irradiation. The above expression is obtained using first-order time-dependent perturbation theory and it is valid for $P_{\mathrm{exc}} \ll 1$. Assuming the laser intensity to be $I = 1$ mW/cm^2 and an excitation time of $t = 1$ s, and using the reduced $M1$ and $E1$ transition matrix elements given above, we get the isomeric excitation probability to be 3.2×10^{-5} for the $M1$ transition channel by a 148-nm laser, and 9×10^{-3} for the $E1$ transition channel by a 131-nm laser.

This 2-orders-of-magnitude enhancement in isomeric excitation can be helpful in the development of $^{229}Th^{3+}$-based ionic nuclear clock. The ionic nuclear clock is expected to achieve the highest precision, however, it is also extremely challenging to obtain nuclear excitation signals due to the very limited number of confined ions. Therefore, it is desirable to obtain $^{229m}Th^{3+}$ with as high efficiency as possible for subsequent spectroscopic investigations. It is to be emphasize that the isomeric frequency in the $^{229}Th^{3+}$ ionic state is different from the frequency determined in doped crystals [26–28]. In the latter case it is mostly in the $^{229}Th^{4+}$ ionic state. Dzuba and Flambaum estimate that an additional electron can cause a nuclear transition frequency shift by 0.1–1 GHz [62].

The transition energy of 9.497 eV (131 nm) is close to the sixth harmonic of Ti:sapphire lasers (800 nm/6 = 133 nm). It may be generated using nonlinear optical processes by adding two third harmonic (266 nm) photons (or a four wave mixing process similar to Refs. [26,27]).

The $E1$ destination state $|I_m, 6d_{3/2}\rangle_+$ quickly decays into the $|I_m, 5f_{5/2}\rangle_+$ state via a purely electronic $E1$

TABLE II. $E1$ decay channels opened by the NHM effect and the corresponding decay rates. The decay rate shown in each row is the total rate of the possible final hyperfine levels.

Initial level	Final levels	Decay rate (s^{-1})
$\lvert I_m, 5f_{5/2}\rangle_+$ $(F=1)$	$\lvert I_g, 6d_{5/2}\rangle_+$ $(F=0,\,1,\,2)$	4.2×10^{-7}
$\lvert I_m, 5f_{5/2}\rangle_+$ $(F=1)$	$\lvert I_g, 6d_{3/2}\rangle_+$ $(F=1,\,2)$	3.0×10^{-6}
$\lvert I_m, 5f_{5/2}\rangle_+$ $(F=1)$	$\lvert I_g, 7s_{1/2}\rangle_+$ $(F=2)$	5.9×10^{-8}
$\lvert I_m, 5f_{5/2}\rangle_+$ $(F=2)$	$\lvert I_g, 6d_{5/2}\rangle_+$ $(F=1,\,2,\,3)$	2.7×10^{-7}
$\lvert I_m, 5f_{5/2}\rangle_+$ $(F=2)$	$\lvert I_g, 6d_{3/2}\rangle_+$ $(F=1,\,2,\,3)$	8.1×10^{-6}
$\lvert I_m, 5f_{5/2}\rangle_+$ $(F=2)$	$\lvert I_g, 7s_{1/2}\rangle_+$ $(F=2,\,3)$	3.6×10^{-7}
$\lvert I_m, 5f_{5/2}\rangle_+$ $(F=3)$	$\lvert I_g, 6d_{5/2}\rangle_+$ $(F=2,\,3,\,4)$	3.5×10^{-7}
$\lvert I_m, 5f_{5/2}\rangle_+$ $(F=3)$	$\lvert I_g, 6d_{3/2}\rangle_+$ $(F=2,\,3,\,4)$	8.5×10^{-6}
$\lvert I_m, 5f_{5/2}\rangle_+$ $(F=3)$	$\lvert I_g, 7s_{1/2}\rangle_+$ $(F=2,\,3)$	6.5×10^{-7}
$\lvert I_m, 5f_{5/2}\rangle_+$ $(F=4)$	$\lvert I_g, 6d_{5/2}\rangle_+$ $(F=3,\,4,\,5)$	6.8×10^{-7}
$\lvert I_m, 5f_{5/2}\rangle_+$ $(F=4)$	$\lvert I_g, 6d_{3/2}\rangle_+$ $(F=3,\,4)$	6.3×10^{-7}
$\lvert I_m, 5f_{5/2}\rangle_+$ $(F=4)$	$\lvert I_g, 7s_{1/2}\rangle_+$ $(F=3)$	1.2×10^{-7}

spontaneous-emission process (Fig. 1). The lifetime of the former state is calculated to be 36.3 μs. The lifetime of the latter state is on the order of 10^3 s. The possibility of population inversion exists between the $|I_m, 5f_{5/2}\rangle_+$ state and the $|I_g, 5f_{5/2}\rangle_+$ state, if the $E1$ pumping rate is higher than the decaying rate of the $|I_m, 5f_{5/2}\rangle_+$ state. For example, with the laser parameters mentioned above (131 nm, 1 mW/cm^2), the pumping rate has already reached 9×10^{-3}, which is higher than the decay rate of the $|I_g, 5f_{5/2}\rangle_+$ state. We would present more elaborated results on this point in a separate publication.

Accelerated decay of the isomeric state—Not only new $E1$ nuclear excitation channels are opened by the NHM effect, new $E1$ decay channels are also opened that modify the decay rate (lifetime) of the isomeric state, hence the stability of the potential ionic nuclear clock. For example, Fig. 1 shows the opened $E1$ decay channel from $|I_m, 5f_{5/2}\rangle_+$ to $|I_g, 6d_{3/2}\rangle_+$. In Table II we list all the opened $E1$ decay channels for each of the hyperfine level ($F=1, 2, 3, 4$) of the $|I_m, 5f_{5/2}\rangle_+$ state. The decay rate is calculated using the following formula [40,42,56]

$$\Gamma(|i\rangle_+ \to |f\rangle_+) = \frac{16\pi k^3}{9(2F_i+1)} |{}_+\langle f\|\mathcal{M}^{(E1)}\|i\rangle_+|^2, \qquad (12)$$

where F_i is the total angular momentum quantum number of the initial state, and k is wave number of the emitted photon.

The decay rate of the bare nucleus is 1.36×10^{-4} s^{-1} using the $B(M1)$ value given earlier. For each hyperfine level, the newly opened $E1$ decay channels result in an additional decay rate. For the $F=1$ level, the total additional $E1$ decay rate amounts to 3.5×10^{-6} s^{-1} (summing the first three rows of Table II), which is 2.6% of the decay rate of the bare nucleus. For the $F=2$ level, the additional $E1$ decay rate is 8.7×10^{-6} s^{-1}, which is 6.4% of the decay rate of the bare nucleus. For the $F=3$ level, the additional $E1$ decay rate is 9.5×10^{-6} s^{-1}, which is 7% of the decay rate of the bare nucleus. For the $F=4$ level, the additional $E1$ decay rate is 1.43×10^{-6} s^{-1}, which is 1.1% of the decay rate of the bare nucleus. This additional $E1$ decay rate leads to a broadening of the isomeric linewidth, hence a decrease of the stability of the potential ionic nuclear clock. We see that the $F=4$ hyperfine level is the least affected one by the NHM effect.

Although the values of $B(M1)$ and $B(E2)$ remain uncertain in the literature ($B(M1)=0.005$–0.048 W.u., $B(E2)=17.55$–42.9 W.u.) [20,58,63,64], the uncertainties mainly affect the magnitude of the decay rate. By contrast, the fractional change in the decay rate is largely insensitive to these uncertainties. With the ranges quoted above, the fractional change for the $F=1$ level varies between 2.5%–2.7%, while the fractional changes for the other three levels remain essentially unchanged.

We note that an electronic bridge (EB) approach has previously been used to predict the accelerated decay of the isomeric state, yielding results of the same order of magnitude [65]. However, that work did not provide hyperfine-level-resolved predictions. This omission arises because the EB approach is formulated using product states of the nucleus and electrons, which are not true eigenstates of the $^{229}Th^{3+}$ ion. The correct eigenstates are total angular momentum states that include hyperfine mixing. Without using these proper eigenstates, one cannot obtain hyperfine-level-resolved predictions or accurately determine the corresponding transition types and rates.

Conclusion—Understanding the role of the electrons is important for the development of the ^{229}Th nuclear clocks, which, after all, are not built on the bare nucleus. In this Letter, we show how the electrons, in particular the single valence electron, would affect the ionic nuclear clock based on $^{229}Th^{3+}$ ions. The NHM effect opens $E1$ transition channels accompanied by nuclear isomeric excitation or decay. On the one hand, the $E1$ channels accelerate decay of the nuclear isomeric state, hence broadening the linewidth and decreasing the stability of the ionic nuclear clock. Depending on the hyperfine level involved, the change in the decay rate is between 1% to 7%. On the other hand, the $E1$ channels can also facilitate more efficient nuclear isomeric excitation. Under the same laser

intensity, a 131-nm laser is 2-orders-of-magnitude more efficient in producing the isomeric state than a 148-nm laser. We believe that these new theoretical insights are important for the development of the ionic nuclear clock.

Acknowledgments—This work was supported by NSFC Grants No. 12474484, No. U2330401, and No. 12088101.

Data availability—The data that support the findings of this article are openly available [66].

[1] L. A. Kroger and C. W. Reich, Features of the low-energy level scheme of ^{229}Th as observed in the α-decay of ^{233}U, Nucl. Phys. **A259**, 26 (1976).

[2] C. W. Reich and R. G. Helmer, Energy separation of the doublet of intrinsic states at the ground state of ^{229}Th, Phys. Rev. Lett. **64**, 271 (1990).

[3] R. G. Helmer and C. W. Reich, An excited state of ^{229}Th at 3.5 eV, Phys. Rev. C **49**, 1845 (1994).

[4] B. R. Beck, J. A. Becker, P. Beiersdorfer, G. V. Brown, K. J. Moody, J. B. Wilhelmy, F. S. Porter, C. A. Kilbourne, and R. L. Kelley, Energy splitting of the ground-state doublet in the nucleus ^{229}Th, Phys. Rev. Lett. **98**, 142501 (2007).

[5] B. Seiferle *et al.*, Energy of the ^{229}Th nuclear clock transition, Nature (London) **573**, 243 (2019).

[6] S. Kraemer *et al.*, Observation of the radiative decay of the ^{229}Th nuclear clock isomer, Nature (London) **617**, 706 (2023).

[7] E. Peik and C. Tamm, Nuclear laser spectroscopy of the 3.5 eV transition in Th-229, Europhys. Lett. **61**, 181 (2003).

[8] V. V. Flambaum, Enhanced effect of temporal variation of the fine structure constant and the strong interaction in ^{229}Th, Phys. Rev. Lett. **97**, 092502 (2006).

[9] K. Beeks, T. Sikorsky, T. Schumm, J. Thielking, M. V. Okhapkin, and E. Peik, The thorium-229 low-energy isomer and the nuclear clock, Nat. Rev. Phys. **3**, 238 (2021).

[10] M. S. Safronova, U. I. Safronova, A. G. Radnaev, C. J. Campbell, and A. Kuzmich, Magnetic dipole and electric quadrupole moments of the ^{229}Th nucleus, Phys. Rev. A **88**, 060501(R) (2013).

[11] B. Seiferle, L. von der Wense, and P. G. Thirolf, Lifetime measurement of the ^{229}Th nuclear isomer, Phys. Rev. Lett. **118**, 042501 (2017).

[12] J. Thielking, M. V. Okhapkin, P. Głowacki, D. M. Meier, L. von der Wense, B. Seiferle, C. E. Düllmann, P. G. Thirolf, and E. Peik, Laser spectroscopic characterization of the nuclear-clock isomer ^{229m}Th, Nature (London) **556**, 321 (2018).

[13] A. Yamaguchi, Y. Shigekawa, H. Haba, H. Kikunaga, K. Shirasaki, M. Wada, and H. Katori, Laser spectroscopy of triply charged ^{229}Th isomer for a nuclear clock, Nature (London) **629**, 62 (2024).

[14] T. Masuda *et al.*, X-ray pumping of the ^{229}Th nuclear clock isomer, Nature (London) **573**, 238 (2019).

[15] P. V. Borisyuk, E. V. Chubunova, N. N. Kolachevsky, Yu. Yu. Lebedinskii, O. S. Vasiliev, and E. V. Tkalya, Excitation of ^{229}Th nuclei in laser plasma: The energy and half-life of the low-lying isomeric state, arXiv:1804.00299.

[16] S. G. Porsev, V. V. Flambaum, E. Peik, and C. Tamm, Excitation of the isomeric ^{229m}Th nuclear state via an electronic bridge process in ^{229}Th^{+}, Phys. Rev. Lett. **105**, 182501 (2010).

[17] P. V. Bilous, H. Bekker, J. C. Berengut, B. Seiferle, L. von der Wense, P. G. Thirolf, T. Pfeifer, Jose R. Crespo López-Urrutia, and A. Pálffy, Electronic bridge excitation in highly charged ^{229}Th ions, Phys. Rev. Lett. **124**, 192502 (2020).

[18] W. Wang, J. Zhou, B. Liu, and X. Wang, Exciting the isomeric ^{229}Th nuclear state via laser-driven electron recollision, Phys. Rev. Lett. **127**, 052501 (2021).

[19] X. Wang, Nuclear excitation of ^{229}Th induced by laser-driven electron recollision, Phys. Rev. C **106**, 024606 (2022).

[20] E. V. Tkalya, Excitation of ^{229m}Th at inelastic scattering of low energy electrons, Phys. Rev. Lett. **124**, 242501 (2020).

[21] H. Zhang, W. Wang, and X. Wang, Nuclear excitation cross section of ^{229}Th via inelastic electron scattering, Phys. Rev. C **106**, 044604 (2022).

[22] J. Qi, H. Zhang, and X. Wang, Isomeric excitation of ^{229}Th in laser-heated clusters, Phys. Rev. Lett. **130**, 112501 (2023).

[23] T. Li, H. Zhang, and X. Wang, Theory of Coulomb excitation of the ^{229}Th nucleus by protons, Phys. Rev. C **108**, L041602 (2023).

[24] J. Zhao, A. Pálffy, C. H. Keitel, and Y. Wu, Efficient production of ^{229m}Th via nuclear excitation by electron capture, Phys. Rev. C **110**, 014330 (2024).

[25] H. Zhang, T. Li, and X. Wang, Highly nonlinear light-nucleus interaction, Phys. Rev. Lett. **133**, 152503 (2024).

[26] J. Tiedau *et al.*, Laser excitation of the Th-229 nucleus, Phys. Rev. Lett. **132**, 182501 (2024).

[27] R. Elwell, C. Schneider, J. Jeet, J. E. S. Terhune, H. W. T. Morgan, A. N. Alexandrova, H. B. Tran Tan, A. Derevianko, and E. R. Hudson, Laser excitation of the ^{229}Th nuclear isomeric transition in a solid-state host, Phys. Rev. Lett. **133**, 013201 (2024).

[28] C. Zhang *et al.*, Frequency ratio of the ^{229m}Th nuclear isomeric transition and the ^{87}Sr atomic clock, Nature (London) **633**, 63 (2024).

[29] W. G. Rellergert, D. DeMille, R. R. Greco, M. P. Hehlen, J. R. Torgerson, and E. R. Hudson, Constraining the evolution of the fundamental constants with a solid-state optical frequency reference based on the ^{229}Th nucleus, Phys. Rev. Lett. **104**, 200802 (2010).

[30] G. A. Kazakov, A. N. Litvinov, V. I. Romanenko, L. P. Yatsenko, A. V. Romanenko, M. Schreitl, G. Winkler, and T. Schumm, Performance of a ^{229}Thorium solid-state nuclear clock, New J. Phys. **14**, 083019 (2012).

[31] B. S. Nickerson, M. Pimon, P. V. Bilous, J. Gugler, K. Beeks, T. Sikorsky, P. Mohn, T. Schumm, and A. Pálffy, Nuclear excitation of the ^{229}Th isomer via defect states in doped crystals, Phys. Rev. Lett. **125**, 032501 (2020).

[32] C. J. Campbell, A. G. Radnaev, and A. Kuzmich, Wigner crystals of ^{229}Th for optical excitation of the nuclear isomer, Phys. Rev. Lett. **106**, 223001 (2011).

[33] C. J. Campbell, A. G. Radnaev, A. Kuzmich, V. A. Dzuba, V. V. Flambaum, and A. Derevianko, Single-ion nuclear clock for metrology at the 19th decimal place, Phys. Rev. Lett. **108**, 120802 (2012).

[34] G. Zitzer, J. Tiedau, C. E. Düllmann, M. V. Okhapkin, and E. Peik, Laser spectroscopy on the hyperfine structure and isotope shift of sympathetically cooled $^{229}Th^{3+}$ ions, Phys. Rev. A **111**, L050802 (2025).

[35] S.-C. Yu, X. Hua, X. Tong, C.-B. Li, and L. She, Highly charged $^{229}Th^{6+}$ ions as the candidate platform for nuclear clock, Chin. Phys. Lett. **42**, 120302 (2025).

[36] L. von der Wense and C. Zhang, Concepts for direct frequency-comb spectroscopy of ^{229m}Th and an internal-conversion-based solid-state nuclear clock, Eur. Phys. J. D **74**, 146 (2020).

[37] R. Elwell *et al.*, Laser-based conversion electron Mössbauer spectroscopy of $^{229}ThO_2$, Nature (London) **648**, 300 (2025).

[38] C. J. Campbell, A. V. Steele, L. R. Churchill, M. V. DePalatis, D. E. Naylor, D. N. Matsukevich, A. Kuzmich, and M. S. Chapman, Multiply charged thorium crystals for nuclear laser spectroscopy, Phys. Rev. Lett. **102**, 233004 (2009).

[39] E. V. Tkalya and A. V. Nikolaev, Magnetic hyperfine structure of the ground-state doublet in highly charged ions $^{229m}Th^{89+,87+}$ and the Bohr-Weisskopf effect, Phys. Rev. C **94**, 014323 (2016).

[40] V. M. Shabaev, D. A. Glazov, A. M. Ryzhkov, C. Brandau, G. Plunien, W. Quint, A. M. Volchkova, and D. V. Zinenko, Ground-state g factor of highly charged ^{229}Th ions: An access to the $M1$ transition probability between the isomeric and ground nuclear states, Phys. Rev. Lett. **128**, 043001 (2022).

[41] J. Jin, H. Bekker, T. Kirschbaum, Y. A. Litvinov, A. Pálffy, J. Sommerfeldt, A. Surzhykov, P. G. Thirolf, and D. Budker, Excitation and probing of low-energy nuclear states at high-energy storage rings, Phys. Rev. Res. **5**, 023134 (2023).

[42] W. Wang and X. Wang, Substantial nuclear hyperfine mixing effect in boronlike ^{205}Pb ions, Phys. Rev. Lett. **133**, 032501 (2024).

[43] K. Beloy, Hyperfine structure in $^{229g}Th^{3+}$ as a probe of the $^{229g}Th \rightarrow {}^{229m}$Th nuclear excitation energy, Phys. Rev. Lett. **112**, 062503 (2014).

[44] V. A. Dzuba and V. V. Flambaum, Shift of nuclear clock transition frequency in ^{229}Th ions due to hyperfine interaction, Phys. Rev. A **108**, 062813 (2023).

[45] W. Wang, F. Zou, S. Fritzsche, and Y. Li, Isomeric population transfer of the ^{229}Th nucleus via hyperfine electronic bridge, Phys. Rev. Lett. **133**, 223001 (2024).

[46] V. L. Lyuboshitz, V. A. Onishchuk, and M. I. Podgoretskij, Some interference phenomena arising by mixing quantum levels in external fields, Sov. J. Nucl. Phys. **3**, 420 (1966).

[47] J. Szerypo, R. Barden, Ł. Kalinowski, R. Kirchner, O. Klepper, A. Płochocki, E. Roeckl, K. Rykaczewski, D. Schardt, and J. Żylicz, Low-lying levels in ^{104}In and a problem of spin-mixing in hyperfine fields, Nucl. Phys. **A507**, 357 (1990).

[48] F. F. Karpeshin, S. Wycech, I. M. Band, M. B. Trzhaskovskaya, M. Pfützner, and J. Żylicz, Rates of transitions between the hyperfine-splitting components of the ground-state and the 3.5 eV isomer in $^{229}Th^{89+}$, Phys. Rev. C **57**, 3085 (1998).

[49] C. Schwartz, Theory of hyperfine structure, Phys. Rev. **97**, 380 (1955).

[50] R. H. Garstang, Hyperfine structure and intercombination line intensities in the spectra of magnesium, zinc, cadmium, and mercury, J. Opt. Soc. Am. **52**, 845 (1962).

[51] P. J. Mohr, Hyperfine quenching of the 2^3P_0 state in heliumlike ions, in *Beam-Foil Spectroscopy*, edited by I. A. Sellin and D. J. Pegg (Springer, Boston, MA, 1976), pp. 97–103.

[52] H. Gould, R. Marrus, and P. J. Mohr, Radiative decay of the 2^3S_1 and 2^3P_2 states of heliumlike vanadium ($Z = 23$) and iron ($Z = 26$), Phys. Rev. Lett. **33**, 676 (1974).

[53] P. Indelicato, F. Parente, and R. Marrus, Effect of the hyperfine structure on the 2^3P_1 and the 2^3P_0 lifetime in heliumlike ions, Phys. Rev. A **40**, 3505 (1989).

[54] R. W. Dunford, C. J. Liu, J. Last, N. BerrahMansour, R. Vondrasek, D. A. Church, and L. J. Curtis, Direct observation of hyperfine quenching of the 2^3P_0 level in heliumlike nickel, Phys. Rev. A **44**, 764 (1991).

[55] P. Indelicato, B. B. Birkett, J. P. Briand, P. Charles, D. D. Dietrich, R. Marrus, and A. Simionovici, Hyperfine quenching and precision measurement of the 2^3P_0-2^3P_1 fine-structure splitting in heliumlike gadolinium (Gd^{62+}), Phys. Rev. Lett. **68**, 1307 (1992).

[56] W. R. Johnson, Hyperfine quenching: Review of experiment and theory, Can. J. Phys. **89**, 429 (2011).

[57] K. T. Cheng, M. H. Chen, and W. R. Johnson, Hyperfine quenching of the 2s2p $^3P_0$ state of berylliumlike ions, Phys. Rev. A **77**, 052504 (2008).

[58] N. Minkov and A. Pálffy, Reduced transition probabilities for the gamma decay of the 7.8 eV isomer in ^{229}Th, Phys. Rev. Lett. **118**, 212501 (2017).

[59] P. Jönsson, G. Gaigalas, J. Bieron, C. F. Fischer, and I. P. Grant, New version: GRASP2K relativistic atomic structure package, Comput. Phys. Commun. **184**, 2197 (2013).

[60] E. Biémont, V. Fivet, and P. Quinet, Relativistic Hartree-Fock and Dirac-Fock atomic structure calculations in Fr-like ions Ra^+, Ac^{2+}, Th^{3+} and U^{5+}, J. Phys. B **37**, 4193 (2004).

[61] Atomic Spectra Database, NIST Standard Reference Database, https://www.nist.gov/pml/atomic-spectra-database (2024).

[62] V. A. Dzuba and V. V. Flambaum, Effects of electrons on nuclear clock transition frequency in ^{229}Th ions, Phys. Rev. Lett. **131**, 263002 (2023).

[63] N. Minkov and A. Pálffy, ^{229m}Th isomer from a nuclear model perspective, Phys. Rev. C **103**, 014313 (2021).

[64] A. M. Dykhne and E. V. Tkalya, $^{229m}Th(3/2^+, 3.5\ \mathrm{eV})$ and a check of the exponentiality of the decay law, JETP Lett. **67**, 549 (1998).

[65] S. G. Porsev and V. V. Flambaum, Effect of atomic electrons on the 7.6-eV nuclear transition in $^{229}Th^{3+}$, Phys. Rev. A **81**, 032504 (2010).

[66] J. Zhou, Figshare (2026), 10.6084/m9.figshare.31420691.v2.